Habilitation Summary of the Scientific Publications

of Senior Assistant Professor Dr. Neda Orlinova Anastasova

for Participation in the Competition for the Academic Position of Associate Professor

in Professional Field 4.2. Chemical Sciences, Scientific Specialty Organic Chemistry,

for the Needs of the Laboratory "Structural Organic Analysis"

The scientific works presented in the habilitation summary fall within the fields of organic and pharmaceutical chemistry, and more specifically, the development of novel potential multitarget agents for the treatment of neurodegenerative diseases. The main scientific contributions result from interdisciplinary research, which can be summarized in the following thematic areas:

1. Design, synthesis, spectral and structural studies of benzimidazole and indole hybrids
2. Investigation of the pharmacological activity of the compounds in various in vitro models
3. Evaluation of the radical-scavenging properties of the compounds in different in vitro systems
4. Conducting in vivo studies in a rat model of dementia
5. Quantum chemical calculations to elucidate the mechanism of action

Introduction

Neurodegenerative diseases represent a heterogeneous group of progressive disorders of the central nervous system, among which Alzheimer's disease (AD) and Parkinson's disease (PD) are the most prevalent. These conditions affect over 60 million people worldwide, including more than 115,000 individuals in Bulgaria. Given the aging population and increasing life expectancy, the number of affected individuals is projected to double by 2050, highlighting the urgent need for the development of new, more effective therapeutic agents capable of addressing this growing challenge [1].

PD is a chronic, progressive, and still incurable disorder characterized by the degeneration of dopaminergic neurons in the substantia nigra pars compacta and the resulting dopamine deficiency in the striatum [2,3]. In addition to the classical motor symptoms (tremor, bradykinesia, rigidity, postural instability), the disease encompasses a broad spectrum of non-motor symptoms such as cognitive impairment, anxiety, depression, sleep disturbances, and autonomic dysfunction, all of which significantly impair patients' quality of life.

Current therapies—including levodopa and its adjuvants, dopamine agonists, MAO-B and COMT inhibitors—provide temporary symptomatic relief but do not target the underlying pathogenic

mechanisms, nor do they slow disease progression. Their effectiveness diminishes over time, and chronic use is associated with serious side effects, necessitating a re-evaluation of the therapeutic approach.

The pathogenesis of PD is highly multifactorial, involving α-synuclein pathology, oxidative stress, mitochondrial dysfunction, neuroinflammation, and biometal dysregulation. Although the primary cause of the disease remains elusive, oxidative stress has been identified as a critical early factor in the neurodegenerative cascade [4]. Increased expression of monoamine oxidase B (MAO-B) and the accumulation of free radicals lead to damage to lipids, proteins, and DNA, promote α-synuclein aggregation, and trigger neuroinflammatory processes [5]. Iron ions further exacerbate these effects through the Fenton reaction and induce ferroptosis. Dopaminergic neurons are particularly reliant on mitochondrial function due to their high energy demands, essential for neurotransmission and plasticity. Mitochondrial impairment is now recognized as a key neurodegenerative mechanism in PD [6].

In this context, the ideal therapeutic candidate should exhibit multimodal activity—namely, MAO-B inhibition, neuroprotective and antioxidant properties, and modulation of mitochondrial and inflammatory pathways. The traditional "one-target" approach is inadequate to address the complexity of the disease, thus driving increasing interest in multi-target therapeutic strategies [7].

The publications presented in this habilitation summary focus on the design, synthesis, and biological evaluation of novel multi-target compounds developed through molecular hybridization of pharmacophores with proven activity. These compounds are directed against key pathogenic mechanisms, with the potential to exert neuroprotective and disease-modifying effects.

I. Synthesis of indole and benzimidazole aryl hydrazones

Publications B1–B5 cover the synthesis and investigation of five series comprising a total of 40 novel arylhydrazone derivatives: **Series I (BIM1):** 1,3-disubstituted benzimidazole-2-thione; **Series II (BIM2):** 1-substituted benzimidazoles; **Series III (IPA):** indole-3-propionic acid derivatives; **Series IV (5MICA):** 5-methoxyindole-2-carboxylic acid derivatives; **Series V (IAA):** indole-3-acetic acid derivatives (Figure 1).These derivatives feature diverse combinations of hydroxyl and methoxy substituents within the arylhydrazone moiety and were investigated as potential multi-target compounds for the treatment of Parkinson's disease. A representative from the 5MICA series, bearing a 3,4-dihydroxy substitution, demonstrated the most promising properties across all in vitro studies and was further evaluated in **in vivo** models of Alzheimer's-type dementia in rats, as reported in publication B3.

The main contribution of the study related to Series I lies in the generation of a broader set of derivatives with varying hydroxy and methoxy substituents on the arylhydrazone fragment. This enabled a comparative analysis and the selection of lead pharmacophoric fragments, which subsequently served as the basis for designing the compounds in Series II–V.

The synthesis of Series I compounds was carried out using a previously developed and optimized methodology. It involves a Michael addition reaction to obtain a disubstituted ester of benzimidazole-2-thione [8], followed by hydrazinolysis and condensation with various hydroxy- and methoxy-substituted benzaldehydes. The other series (II–V) were synthesized in an analogous manner, with the main difference lying in the initial step for obtaining the ester precursor. Structural characterization of the compounds was performed using infrared (IR) spectroscopy, nuclear magnetic resonance spectroscopy (^{1}H and ^{13}C NMR), and high-resolution mass spectrometry (HRMS). Additionally, X-ray crystallographic analysis was carried out for two derivatives from the 5MICA series [Γ5]. Furthermore, quantum chemical calculations were conducted for some compounds to determine the most probable molecular geometries and mechanisms of radical scavenging. DFT methods were also applied in order to be explained the observed in the ^{1}H and ^{13}C NMR spectra duplicated signals of some compounds, suggesting the presence of conformers.

The interdisciplinary investigations allowed a more comprehensive pharmacological evaluation of the synthesized arylhydrazones. The generated experimental data pertain to their cytotoxicity, neuroprotective and antioxidant activities, as well as their ability to inhibit MAO-B. The potential permeability across the blood–brain barrier (BBB) for the compounds from Series III and IV was also examined as an essential property for drug candidates targeting neurodegenerative disorders. As a result of this evaluation, a lead structure with high multi-target potential was identified from Series IV and advanced to in vivo studies [B3].

In view of the interdisciplinary nature of the research and the aim for clearer systematization, the presentation of the results from the publications included in this habilitation report is organized thematically—according to the biological activities studied—in order to trace the pharmacological potential of each series within the context of the respective model.

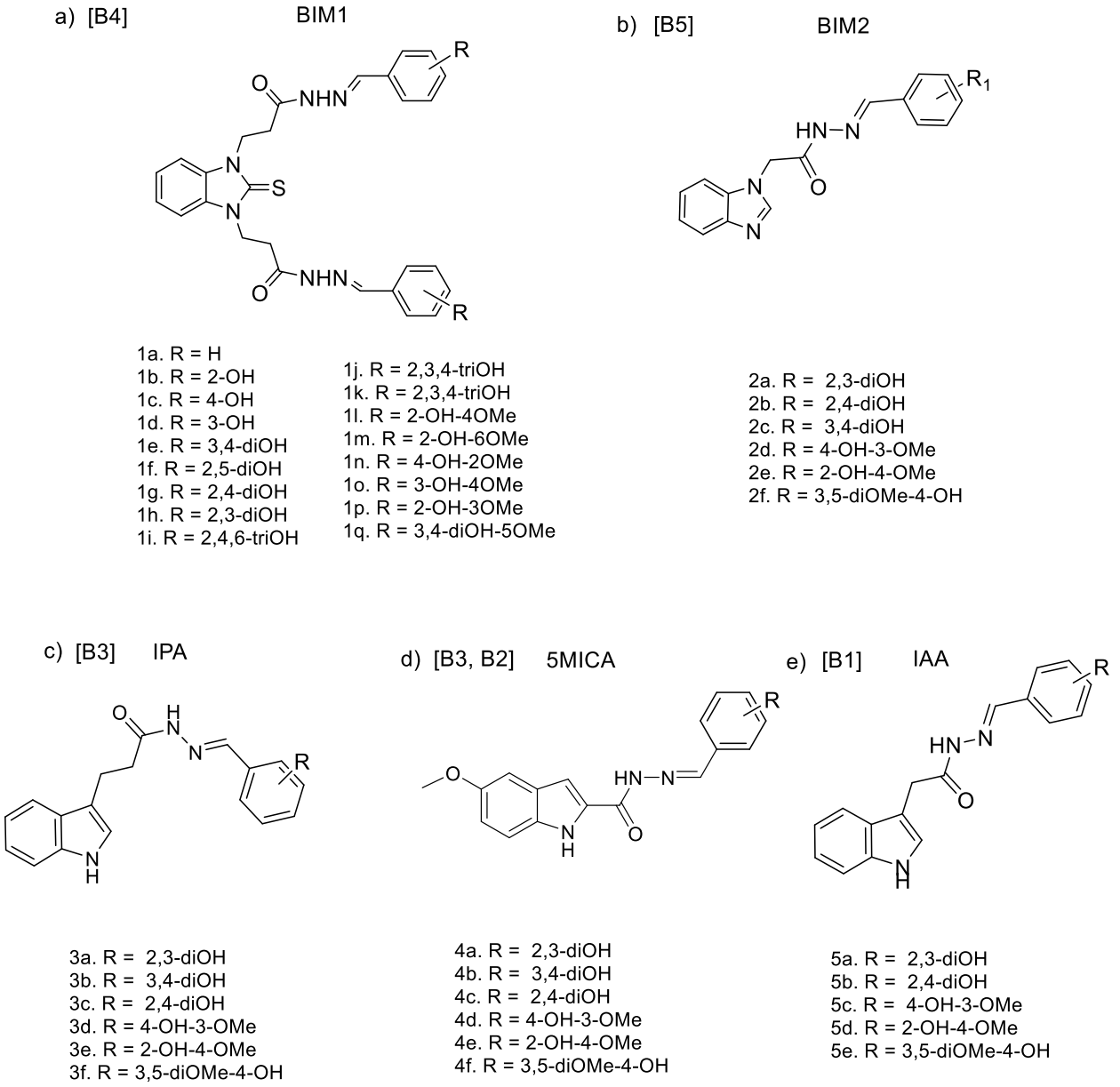

Figure 1. Structures of the compounds investigated in the habilitation work, as follows: a) Series I (BIM1) – N,N′-disubstituted benzimidazole-2-thione arylhydrazones – publication B4; b) Series II (BIM2) – N-substituted benzimidazole arylhydrazones – publication B5; c) Series III (IPA) – arylhydrazones of indole-3-propionic acid – publication B3; d) Series IV (5MICA) – arylhydrazones of 5-methoxyindole carboxylic acid – publications B3, B4; e) Series V (IAA) – arylhydrazones of indole-3-acetic acid – publication B1.

II. Establishing a safety profile

As a key step in the development of novel pharmacologically active compounds, an initial assessment of their safety profile was conducted. The toxicological evaluation involved studies using the SH-SY5Y neuroblastoma cell line, a well-established model in neuroscience research [9]. SH-SY5Y cells are of human origin and exhibit relatively homogeneous neuroblast-like morphology. They express enzymatic activity of dopamine-β-hydroxylase and tyrosine hydroxylase, as well as specific human proteins and their isoforms.

The potential neurotoxic effects of the investigated compounds were evaluated using the cell viability assay (MTT test), with IC_{50} values used as comparative parameters. To extend the toxicological assessment, the experimental approach was expanded with an additional in vitro model using freshly isolated rat brain synaptosomes. This model was considered appropriate, as the synaptosomal fraction contains synaptic vesicles, membranes, neurotransmitters, and part of the postsynaptic membrane, along with both enzymatic forms of monoamine oxidase (MAO-A and MAO-B) [10]. The functional-metabolic status of the synaptosomes was assessed by measuring their viability (MTT test) and reduced glutathione (GSH) levels.

• In the series of disubstituted benzimidazoles (BIM1), cytotoxicity against SH-SY5Y cells varied over a wide range (IC_{50} = 65.30–301.10 μM), with a significant number of compounds demonstrating a favorable safety profile. Eight compounds were identified with the lowest toxicity (IC_{50} > 200–250 μM) and were considered more promising for further biological characterization, namely: **1d** (3,5-dimethoxy-4-hydroxy), **1h** (2,3-dihydroxy), **1i** (2,4-dihydroxy),**1n** (2-hydroxy-6-methoxy),**1p** (4-hydroxy-2-methoxy), **1e** (o-hydroxy), **1l** (2-hydroxy-3-methoxy), and **1m** (2-hydroxy-4-methoxy). On the other hand, substituents associated with higher cytotoxicity were identified (IC_{50} = 65.30–77.79 μM), including compounds:**1f** (m-methoxy), **1g** (p-hydroxy), **1k** (2,3,4-trihydroxy),1o (3-hydroxy-4-methoxy), and **1q** (3,4-dihydroxy-5-methoxy).

In isolated rat synaptosomes, compounds **1e**, **1h**, **1i**, and **1m** at concentrations up to 250 μM did not exhibit significant toxicity and did not reduce GSH levels. Their effects were comparable to those of the reference compound melatonin.

• In the series of monosubstituted benzimidazole hydrazone derivatives (BIM2), the calculated IC_{50} values against SH-SY5Y cells also spanned a wide range (89.23–311.43 μM), indicating significant variability in cytotoxicity depending on the type of substituent. Compounds **2d** (vanillin derivative), **2e** (2-hydroxy-4-methoxy), and **2f** (syringaldehyde derivative) demonstrated the lowest overall toxicity (IC_{50} > 228 μM) and stood out with favorable safety profiles, which was confirmed in the isolated synaptosome model.

The observed preservation of synaptosomal viability and GSH levels at concentrations up to 100 μM for these compounds confirmed their low toxicological potential. At 50 μM, they did not induce significant changes in either of the analyzed parameters. Compounds **2d** and **2e** were identified as

the representatives with the best safety profile within this series and were thus designated as priority candidates for further biological evaluation.

• To assess the biocompatibility of the indole-based compounds from the IPA and 5MICA series, an additional model was employed—a hemolysis assay, which is based on the release of hemoglobin from erythrocytes as a marker of cellular lysis. At all tested concentrations, including the highest (200 μM), the compounds did not induce significant hemolytic effects (< 5%). Cytotoxicity evaluation using the SH-SY5Y cell model revealed that indole-3-propionic acid derivatives **3e** and **3f** exhibited very low toxicity (IC_{50} > 500 μM). Somewhat higher but still low toxicity was observed for compounds **3b** (265.3 μM), **3c** (275.2 μM), and **4f** (286.9 μM), whereas **4a**, **4c**, and **4d** showed more pronounced cytotoxicity, with IC_{50} values below 100 μM. In the synaptosomal model, compounds from series **4a**–**f** exhibited a less pronounced reduction in cellular viability (25–30%) compared to the IPA derivatives, where the effect was approximately 40%. In most cases, the decline in GSH levels was within the range of 20–25%.

• The IAA derivatives also demonstrated a favorable safety profile. The lowest cytotoxicity was recorded for compounds **5a**, **5b**, and **5e** (IC_{50} > 140 μM). When applied at a concentration of 100 μM, all compounds from this series caused a moderate reduction in synaptosomal viability (30–35%) and in GSH levels (15–20%) compared to untreated controls.

Considering the key role of mitochondrial function in the survival of dopaminergic neurons and its involvement in the pathogenesis of Parkinson's disease, an evaluation of the effects of selected compounds from the IAA series was performed on mitochondria isolated from rat brain. At a concentration of 100 μM, statistically significant but relatively mild changes were observed in the levels of malondialdehyde (MDA)—a marker of lipid peroxidation—and GSH.

The most pronounced changes were recorded for compounds **5a** and **5d**, which induced a 30–32% increase in MDA and a reduction in GSH of approximately 15%. For the remaining compounds (**3b**, **3c**, and **3e**), the increase in MDA ranged from 36% to 39%, while the reduction in GSH ranged from 10% to 15% compared to untreated controls. These findings indicated the presence of some prooxidant activity, but did not exclude them potential applicability.

Additionally, an in vitro evaluation of the compounds from this series was carried out using a model with isolated brain microsomes, again by measuring MDA levels. At a concentration of 100 μM, a moderate increase in MDA in the range of 18–26% compared to the control was observed, with the lowest prooxidant activity found for the 2,3-dihydroxy derivative **5a**.The compounds from this series exhibited low to moderate toxicity, with **5a** and **5d** showing a more favorable profile compared to **5c** and **5e**. The compound **5a**, bearing 2,3-dihydroxy substituents, stood out with the weakest prooxidant effect.

Despite the observed effects, it was concluded that the compounds possess low toxicological potential, and the effects observed do not significantly compromise the therapeutic potential of the

indole derivatives—especially in light of their pronounced neuroprotective and antioxidant activity, as evaluated in the subsequent experimental models.

A key contribution of this work is the toxicological evaluation of newly synthesized compounds from five series of arylhydrazones, using several in vitro models. Compounds with the most favorable safety profiles and lowest cytotoxicity were identified and selected as priority candidates for further biological evaluation.

III. Studies on neuroprotective activity

III.1. Model of H_2O_2-induced oxidative stress in SH-SY5Y cells

To evaluate the potential of the studied compounds as neuroprotective agents, a well-established cellular model of hydrogen peroxide-induced oxidative stress was employed, using the human neuroblastoma cell line SH-SY5Y. H_2O_2 is a low-molecular-weight oxidant that easily permeates the cell membrane and, in the presence of divalent metal ions, generates reactive oxygen species (ROS), including hydroxyl and peroxyl radicals which damage cellular components such as DNA, proteins, and lipids, ultimately leading to dysfunction and cell death. This model enables the assessment of a compound's ability to prevent oxidative injury, with cell viability measured by the MTT assay. SH-SY5Y cells were pre-treated with various concentrations of the compounds, followed by induction of oxidative stress with H_2O_2.

• From the disubstituted benzimidazoles in Series I, selected compounds with previously established low toxicity (**1d**, **1e**, **1h**, **1i**, **1m**, **1n**, and **1p**) were investigated. Cells were pre-incubated with concentrations of 1, 10, and 50 μM, followed by treatment with H_2O_2 (1 mM). The resulting data indicated that all tested compounds exhibited varying degrees of protective effect. As reference compounds, melatonin and rasagiline—both known for their neuroprotective properties—were used. Treatment with melatonin at concentrations of 1, 10, and 50 μM resulted in increased cell viability by 20%, 29%, and 52%, respectively, while rasagiline produced increases of 10%, 20%, and 39%.

Among the disubstituted benzimidazoles, compounds **1h (**2,3-dihydroxy) and **1i** (2,4-dihydroxy) demonstrated the most pronounced neuroprotective effects, with 50 μM treatments increasing cell viability to 79% and 80%, respectively. These values significantly exceeded the effects of the reference compounds at the same dose, supporting the role of phenolic groups in the mechanism of action likely through direct ROS scavenging and stabilization of intracellular redox homeostasis. These findings suggest that certain disubstituted benzimidazole derivatives possess significant neuroprotective potential in this cellular model.

• Among the monosubstituted benzimidazole derivatives from Series II, only pretreatment with compound **2e** (2-hydroxy-4-methoxy) led to a significant reduction of H_2O_2-induced cellular damage. A statistically significant, concentration-dependent neuroprotective effect was observed,

with cell viability increasing by 18%, 71%, and 60% at concentrations of 1, 10, and 25 μM, respectively, compared to the H_2O_2-treated control group. The neuroprotective activity of this compound was further confirmed through microscopic analysis, which revealed preserved cellular morphology compared to the pronounced damage observed in cells treated only with H_2O_2.

Thus, compound **2e** demonstrated superior efficacy at all tested concentrations compared to the reference neuroprotective compounds melatonin and rasagiline, highlighting its potential as a lead structure for further pharmacological development.

• All compounds from the IPA and 5MICA series exhibited strong neuroprotective activity at low concentrations (1 and 10 μM), in some cases restoring cell viability up to 80%, significantly surpassing the activity of the reference compounds melatonin and rasagiline, which indicates the high protective potential of the synthesized derivatives. The strongest effect was observed for compounds containing catechol groups and vinylic fragments. A similar trend was established for the IAA series, where the derivative with a 2,3-dihydroxy substituent (compound **5a**) showed the most potent protective effect (68% cell viability), exceeding the activity of both the other compounds in the series and the reference agents.

An interesting observation was the fact that, while the catechol moiety (2,3-dihydroxy) appeared to be a key structural determinant of neuroprotective activity among the disubstituted benzimidazole arylhydrazones and indole derivatives from the IPA and IAA series, in the case of monosubstituted benzimidazoles, the most pronounced activity was exhibited by compound **2e**, which contains a 2-hydroxy-4-methoxy substitution pattern. This deviation from the general structure-activity trend was the subject of a dedicated publication [Γ2], where extensive quantum chemical calculations were employed to rationalize the observed activity (see Section V).

In summary, the obtained results clearly demonstrated a structure–activity relationship between the synthesized molecules and their biological activity. Some of the studied compounds were identified as promising candidates for further investigation as neuroprotective agents, based on their effectiveness under conditions of induced oxidative stress, a key pathogenic mechanism in neurodegenerative disorders.

III.2. 6-OHDA-Induced neurotoxicity in isolated rat brain synaptosomes

The neuroprotective potential of the compounds was further assessed in a model of 6-hydroxydopamine (6-OHDA)-induced neurotoxicity using synaptosomes isolated from rat brain. Due to its selective affinity for the dopamine transporter, 6-OHDA enters dopaminergic neurons where it undergoes autooxidation and is metabolized by monoamine oxidase B (MAO-B) to reactive intermediates, including p-quinone. This leads to the intense formation of reactive oxygen species (ROS), mitochondrial dysfunction, and depletion of intracellular glutathione (GSH). Application of 6-OHDA at a concentration of 150 μM resulted in the expected reduction of both cell viability and GSH levels by approximately 50% compared to the untreated control group.

• In the disubstituted benzimidazole series (Series I), four compounds were studied - **1e** (o-OH), **1h** (2,3-dihydroxy), **1i** (2,4-dihydroxy), and **1m** (2-OH-4-OMe) which, at a concentration of 10 μM, demonstrated varying degrees of protection. The most pronounced effect was observed with compound **1h**, which restored cell viability and GSH levels to 71% and 62%, respectively. This effect was comparable to that of the reference compounds melatonin and rasagiline. The remaining derivatives also exhibited statistically significant, albeit lower, neuroprotective activity.

• In the N-alkylated benzimidazole series, compound **2e** (10 μM) exhibited distinct neuroprotective activity in the 6-OHDA model, as evidenced by a 35% recovery of synaptosomal viability and a 55% increase in GSH levels compared to the 6-OHDA control. These values were higher than those of rasagiline and comparable to the effects of melatonin, further underscoring the potential of compound **2e** as an effective antioxidant and neuroprotective agent.

• The studied indole derivatives from the IPA and 5MICA series, applied at a concentration of 10 μM, also showed statistically significant effects. Among them, compounds **3a**, **3f**, **4b**, **4c**, and **4d** restored synaptosomal viability by approximately 44%, while 3b–3e restored it by about 33%. Regarding GSH levels, the protective effect of most compounds was comparable to that of the reference indole-3-propionic acid. The highest degree of protection of the functional–metabolic status of synaptosomes was observed with compounds **4a** (2,3-dihydroxy), **4e** (2-hydroxy-4-methoxy), and **4f** (3,5-dimethoxy-4-hydroxy) which restored viability up to 56%.

• As for the IAA series, the most pronounced neuroprotection was demonstrated by compounds **5b** (2,4-dihydroxy) and **5c** (vanillin derivative) which preserved both synaptosomal viability and GSH levels by 36% and 80%, respectively, compared to 6-OHDA. Similar, though less pronounced, effects were observed for compounds **5a** (2,3-dihydroxy) and **5e** (3,5-dimethoxy-4-hydroxy), with 33% and 50% protection, respectively. Compound **5d** (2-hydroxy-4-methoxy) also showed moderate protective activity.

The obtained data supported the results from the H_2O_2-induced cellular model and expanded the neuroprotective profile of the studied compounds.

III.3. Neuroprotective activity in isolated mitochondria and microsomes [B1]:

The profile of the compounds from the IAA series was further extended by evaluating their neuroprotective effects in a model of t-BuOOH-induced oxidative stress in isolated rat brain mitochondria. t-Butyl hydroperoxide (t-BuOOH) induces significant neurotoxicity, manifested by a decrease in GSH levels and an increase in MDA content. The most pronounced activity was once again observed for compound **5a**, which demonstrated the strongest neuroprotective effect, preserving up to 80% of GSH levels and reducing MDA concentration by 37% compared to the t-BuOOH-treated group. The other compounds from the series also showed protective effects, maintaining GSH levels between 50–60% and reducing MDA production by 13–24%.

Additionally, the compounds from this series were evaluated in a model of oxidative stress in isolated microsomes, in which lipid peroxidation was induced by a combination of iron and ascorbic acid, triggering a Fenton reaction and the generation of hydroxyl radicals (•OH). As a result, a 139% increase in MDA production was observed compared to the control group. Once again, compound **5a** stood out with the most potent antioxidant activity, reducing MDA levels by 46% relative to the toxic agent. The remaining compounds showed a protective effect in the range of 23% to 34% MDA reduction.

The obtained data supported the significant antioxidant and neuroprotective potential of the 2,3-dihydroxy derivative **5a**, demonstrated across various subcellular fractions.

The main contributions from the neuroprotection studies lie in the elucidation of structure–activity relationships for the manifestation of neuroprotective effects and the identification of lead structures that outperform the reference compounds.

III.4. Evaluation of MAO-B inhibitory activity

The inhibitory potential of the investigated compounds was assessed against the human recombinant enzyme hMAO-B using a fluorometric assay with Amplex UltraRed as the detection dye.

Selected disubstituted benzimidazoles with established safety profiles and pronounced neuroprotective properties (**1d**, **1e**, **1h**, **1i**, **1m**, **1n**, **1p**) were tested at a concentration of 1 μM and compared to the clinically used MAO-B inhibitors, selegiline and rasagiline. All compounds exhibited statistically significant inhibitory activity, with compound 1h, containing a catechol moiety, showing the most potent effect, comparable to that of the reference inhibitors. Molecular docking studies supported the experimental findings, revealing that the hydrazone side chains attached to the nitrogen atoms of the benzimidazole core enhance the ligand fit within the narrow, highly lipophilic cavity of the MAO-B active site, facilitating stronger interactions with key amino acid residues. The flexibility of the ligands allows them to adopt conformations favorable for effective binding within the active site.

• Among the monosubstituted benzimidazoles from Series II, all tested compounds demonstrated statistically significant MAO-B inhibitory activity, with compound **2e** exhibiting a noteworthy effect, reducing hMAO-B activity by 65%, comparable to the classical inhibitors selegiline and rasagiline. This result, combined with its low cytotoxicity and strong neuroprotective activity, positions compound 2• e as a promising candidate for the development of multi-target therapy for PD. Supporting the experimental data, molecular docking revealed that, unlike the other compounds, **2e** is capable of reaching in close proximity to the FAD cofactor, thanks to a favorable geometry that allows deeper penetration into the enzyme's active-site cavity. Stabilizing hydrogen bonds were observed between **2e** and the Tyr326 residue, a key residue located in the polar region between the entrance cavity and the catalytic site. In addition, **2e** formed the strongest hydrogen

bonding interactions with Cys172. The other compounds failed to achieve such favorable positioning due to the lipophilic nature of the catalytic cavity, which repels hydroxy (OH) and methoxy (OMe) substituents. Furthermore, steric hindrance at the entrance cavity—caused by bulkier substituents further limits binding. These observations are consistent with the experimentally established high inhibitory activity of compound **2e** and confirm its affinity for MAO-B (see Fig. 2).

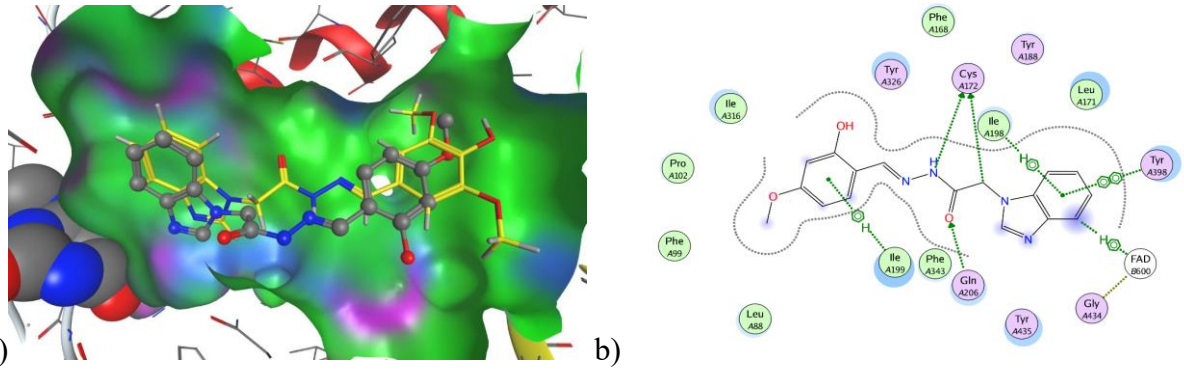

Figure 2. The most favorable interacting derivative **2e** inside the MAO-B pocket. (A) Derivative **2e** (represented with gray carbons) compared to **2f** (represented with yellow carbons) derivative inside the MAO-B active site pocket. The distant side of the pocket is represented from van der Waals (vdW) radii; lipophilic parts are depicted in green; polar are in pink and blue color. The closest part of flavine cofactor is seen on the left, with atoms represented as van der Waals spheres. (B) Schematic depiction of the close proximity to the most active derivative **2e** inside the MAO-B pocket. MAO-B:

• All tested compounds from the IPA and 5MICA series (1 μM) exhibited statistically significant inhibitory activity against hMAO-B. Representatives of the 5MICA group reduced enzymatic activity by approximately 35–40%, while compounds from the IPA group showed a reduction of around 20%. Molecular docking revealed that all compounds adopt planar conformations that allow effective positioning within the hydrophobic active site of the enzyme.

•Regarding the IAA series, all compounds were found to inhibit MAO-B in the submicromolar range (IC_{50} = 0.130–0.493 μM), with compounds 5d, 5e, and 5a demonstrating selectivity toward MAO-B over MAO-A. The binding of the synthesized ligands to both MAO-B and MAO-A isoforms was examined using molecular docking. The results indicated that all investigated compounds exhibited stronger binding energies with MAO-B, confirming it as the preferred target. The lowest (i.e., most favorable) binding energy was observed for compound **5e**, while the other compounds showed similar values with a gradual decrease in binding affinity. Due to their extended linear structures, the compounds fit well into the narrow and elongated active site of MAO-B without significant steric hindrance. All ligands were found to occupy both the entrance channel and substrate cavity of the MAO-B active site, settling into the flat hydrophobic region

characteristic of the enzyme. Analysis of the top 10 poses for MAO-B revealed that all ligands formed van der Waals interactions with Tyr398 and Tyr435, which constitute the so-called "aromatic cage", as well as with Leu171. Additionally, interactions with Phe343, Ile316, and Tyr60 were also mediated via van der Waals forces, while hydrogen bonds were formed with Ile199 through the amide group and Gln206(via the side chain.

Selectivity toward MAO-B is a key consideration in the development of inhibitors for the treatment of neurodegenerative disorders such as Parkinson's and Alzheimer's disease. The lack of MAO-A inhibition reduces the risk of side effects related to increased levels of serotonin and noradrenaline. In this context, the identification of three MAO-B selective inhibitors **5a**, **5d**, and **5e** represented a significant contribution, highlighting the potential of hydrazone derivatives of indole-3-propionic acid as promising scaffolds for the development of new neuroprotective agents.

In publication B3, the potential effects of compounds from the IPA and 5MICA series on the blood–brain barrier (BBB) were evaluated using a static model based on the bEnd3 endothelial cell line. These cells express tight junction proteins such as ZO-1 and claudin-5, which are critical for maintaining intercellular barrier integrity. Compounds **3d**, **3e**, and 3f were found to increase permeability at a concentration of 10 μM without disrupting the tight junctions. Compound **4e** significantly increased permeability but compromised junctional integrity and was therefore excluded from further investigations. Conversely, the two dihydroxylated derivatives, **4a** and **4b**, demonstrated favorable properties enhancing permeability without damaging the endothelial monolayer.

Based on the results from the combined in vitro evaluations, compound **4b** was selected for in vivo characterization, which became the focus of publication B2.

IV. In vitro studies on radical-scavenging properties

Neuronal tissue is characterized by high oxygen consumption and the presence of polyunsaturated fatty acids, which are highly susceptible to oxidative damage. The accumulation of lipid peroxidation markers such as malondialdehyde and lipid hydroperoxides in patients at early stages of Parkinson's disease underscores the need for therapeutic strategies that address not only the dopaminergic deficit but also the restoration of redox homeostasis [10].
In this context, the radical-scavenging properties of benzimidazole and indole-based hybrids were investigated using various in vitro models. The results clearly demonstrated a structure-dependent effect on antioxidant activity.

IV.1. Inhibition of Fe(II)-induced lecithin and deoxyribose damage

•Among the disubstituted benzimidazoles, the strongest antioxidant effects were observed for compounds **1d** (syringaldehyde derivative), **1h** and **1j** (catechol derivatives), and **1q** (3,4-

dihydroxy-5-methoxy). These compounds reduced absorption to about 40% of control, indicating a high efficiency in suppressing lipid peroxidation. In the deoxyribose degradation model, compound **1h** (2,3-dihydroxy) also exhibited strong protective effects, exceeding those of melatonin and comparable to Trolox.

•Among the N-alkylated benzimidazoles from Series II, all tested compounds were capable of suppressing lipid peroxidation. Notably, compounds **2b**, **2d**, **2e**, and **2f** showed similar protective effects, reducing damage to 63–65% of control, while compounds **2a** and **2c** displayed the strongest protection, with values of 38.88% and 47.52%, respectively—placing them among the most effective inhibitors of oxidative lecithin degradation in the model.

•In a model system containing lecithin, all tested indole derivatives from the IPA (**3a**–**f**) and 5MICA (**4a**–**f**) series inhibited iron-induced lipid peroxidation, with antioxidant activity corresponding to absorption coefficients between 30–75% relative to control. The most effective were the 2,3-dihydroxylated derivatives, **3a** and **4a** (~30%), exhibiting activity comparable to the reference antioxidant Trolox. Similarly, within the IAA series, the 2,3-dihydroxylated derivative **5a** (54%) showed the most pronounced effect, reaffirming the key role of the catechol moiety in antioxidant action. In the deoxyribose assay for protection against iron-induced oxidative damage, most compounds exhibited antioxidant effects. Compounds **3b**, **3f**, **4b**, and 4f displayed effectiveness statistically equivalent to Trolox, while compound 4a demonstrated activity comparable to quercetin (~50%).
The highest antioxidant activity among the IPA series was observed for compound 3a, exceeding that of quercetin.

In this study as well, compound **5a** from the IAA series demonstrated the highest antioxidant activity among all tested derivatives (53.6%), surpassing the effect of Trolox, further reinforcing its potential as a potent antioxidant.

IV.2. Evaluation of superoxide and hypochlorite radical scavenging capacity
The investigation of radical-scavenging activity against superoxide anions and hypochlorite ions is motivated by their pivotal role in oxidative stress, neuroinflammation, and neuronal damage associated with neurodegenerative diseases. These species participate in dopamine autooxidation and the formation of toxic quinones, which deplete intracellular NADPH and contribute to cell death [11,12].

The compounds' ability to scavenge superoxide radicals was assessed using the xanthine/xanthine oxidase enzymatic system. Most tested compounds showed only modest decreases in absorbance compared to the control, corresponding to weak inhibition of superoxide generation. The presence of two hydroxyl groups was found to enhance radical-scavenging ability in this model.

•Among the disubstituted benzimidazoles, the salicylic acid derivative **1e** and 2-hydroxy-4-methoxy derivative 1m had no statistically significant effect across the tested concentration range. In contrast, compound 1h (2,3-dihydroxy) demonstrated the most pronounced activity, reducing absorbance to 64% of control. Compound 3i induced a moderate effect (15%).
•In the indole series (5MICA and IPA), the highest activity was observed for the two 3,4-dihydroxylated derivatives. In the presence of compound 3b (100 μM), absorbance decreased by over 40%, while compound 4b showed even greater activity, reducing the signal to 20% at a tenfold lower concentration.
•In the IAA series, the 2,3-dihydroxylated compound 5a exhibited strong, concentration-dependent scavenging of superoxide anions, reaching up to 87% activity at 10 μM. In contrast, compounds **5c** and **5d** showed no activity at any tested concentration. The 2,4-dihydroxy derivative **3b** displayed weaker but statistically significant absorbance reduction only at the highest tested concentration (25 μM).

•The ability to scavenge hypochlorite anions (ClO^-) was also assessed for the IAA series. All compounds, with the exception of the 2-hydroxy-4-methoxy derivative (**5d**), demonstrated concentration-dependent activity, where increasing compound concentration correlated with enhanced radical-scavenging effects. A linear concentration-activity relationship was observed for two dihydroxy derivatives—**5a** and **5b**—as well as the syringaldehyde-containing compound **5e**. The vanillin derivative **5c** exhibited saturation of radical-scavenging capacity at concentrations above 40 μM, with only modest but statistically significant changes in the measured parameter. The most active compound, **5a** (2,3-dihydroxy derivative), achieved over 50% ClO^- scavenging at the maximum tested concentration of 25 μM.

IV.3. Evaluation of Fe(III) reducing capacity

Considering the role of iron-induced lipid peroxidation in neurodegenerative processes, particularly in the pathophysiology of the substantia nigra in Parkinson's disease, the antioxidant activity of hydrazone derivatives from the IAA series was evaluated. The redox balance between Fe(III)/Fe(II) is critical in limiting oxidative damage, including the initiation of Fenton reactions and the subsequent generation of highly reactive hydroxyl radicals.Most of the tested compounds showed statistically significant effects, with a reduction effect of approximately 20% already at the lowest tested concentration (2.5 μM). At the maximum concentration of 20 μM, the activity reached up to 80%, indicating strong Fe(III)-reducing capacity.

Based on the obtained results from the radical-scavenging activity assays, a more in-depth understanding of the structure–activity relationships governing the antioxidant potential of hydrazone side chain substituents was achieved. The data confirmed the crucial role of the catechol moiety in eliciting potent antioxidant effects—both in biologically relevant systems such as lecithin and deoxyribose, and in assays involving diverse reactive oxygen species.

V. DFT studies

To further clarify the superior neuroprotective activity of the 2-hydroxy-4-methoxy derivative **2e** compared to the 2,3-dihydroxy analogue **2a** (as reported in publication B5), quantum chemical calculations were carried out to investigate the most probable mechanisms of free radical scavenging. The pathways explored included formal hydrogen atom transfer (fHAT), single electron transfer (SET), and radical adduct formation (RAF), modeled in both polar (water) and non-polar (benzene) environments. The results, published in contribution G2, demonstrated that the fHAT mechanism is the predominant pathway for deactivation of •OH, •OCH_3, and •OOH radicals. In aqueous solution, the most reactive positions for fHAT were found to be H28 in compound **2a** (99.33%) and H25 in **2e** (99.68%) [Fig. 3]. The same positions were confirmed as the most reactive in the benzene environment. Further investigation into the radical-scavenging mechanisms of •OCH_3 in non-polar medium revealed that in compound 2a, the amide N–H group reacts approximately two orders of magnitude faster than the phenolic O22–H28 group, highlighting its key contribution to the radical deactivation process.

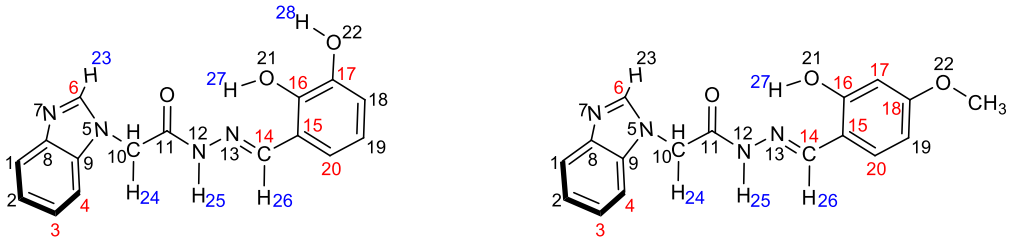

Figure 3. Possible sites for hydrogen atom transfer (fHAT) (in blue) and radical adduct formation (RAF) (in red) for compounds **2a** and **2e**

The computational data indicated that scavenging of the •OOH radical is feasible exclusively via the fHAT mechanism, with compound **2e** demonstrating approximately 100-fold higher reactivity than 2a in non-polar environment. The SET pathway was excluded as a plausible mechanism in both polar and non-polar media.

NBO analyses revealed that the spin density in the radical species formed after hydrogen abstraction from the amide N–H group is delocalized over the aromatic ring and the hydrazone moiety. The higher degree of delocalization observed in the radical form of compound **2e** (R2eN12) is consistent with its theoretically predicted higher radical-scavenging potential, as well as with the experimentally confirmed superior neuroprotective activity [Figure 4].

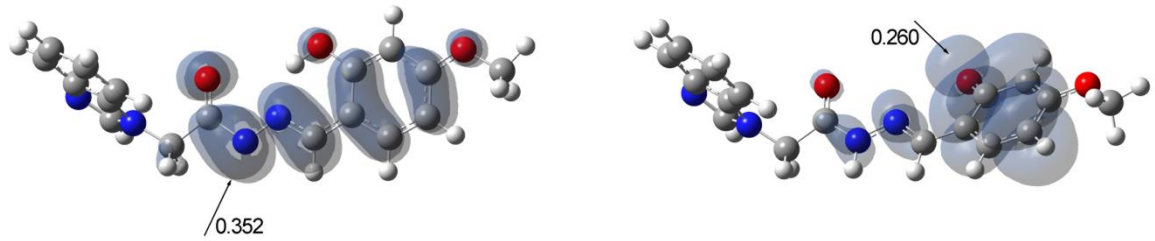

R2e N12 **R2e O21**

Figure 4. Electron density distribution in the two most stable radical species of 2e, calculated at the (U)M06-2X/6-311++G** level of theory in benzene.

In the NMR spectra of the N,N′-disubstituted arylhydrazone derivatives of benzimidazole-2-thione described in publication B4, signal duplication was observed for several resonances, including those of the methylene protons, the azomethine proton, and the NH group. This behavior is indicative of the presence of conformers in solution. Previous investigations by our group demonstrated the existence of multiple conformers, owing to the rotational flexibility of the N–N bond and the potential E/Z isomerism about the azomethine linkage [14].

Similar duplication of NMR signals was also recorded for the IAA series compounds [B1], with an integral signal ratio of approximately 3:1. To confirm the presence of stable conformers in this case, DFT calculations were performed in DMSO (B3LYP/6-311++G** level of theory). The optimized geometry revealed a planar indole moiety oriented at an angle of 85° relative to the hydrazone chain, with the amide group and azomethine linkage stabilized in trans configuration.

Two main conformers were identified, arising from rotation around the C–C bond between the pyrrole ring and the methylene carbon, with an energy difference (ΔG) in the range of 1.64–3.49 kJ mol^{-1}. In addition, rotation around the N–N bond resulted in the formation of s-cis and s-trans conformers, the latter being considerably more stable (ΔG of 7–11 kJ mol^{-1}), likely due to an intramolecular hydrogen bond between the lone pair on the azomethine nitrogen and the ortho-hydroxyl group of the aryl ring. The Boltzmann distribution, calculated based on the energy differences between conformers, confirmed that the dominant population observed in the NMR spectra corresponds to the E, s-trans conformation. Additional support for the presence of conformers was obtained from variable-temperature ^{1}H NMR spectroscopy: at 80 °C, signal coalescence was observed, attributed to interconversion between conformers in solution.

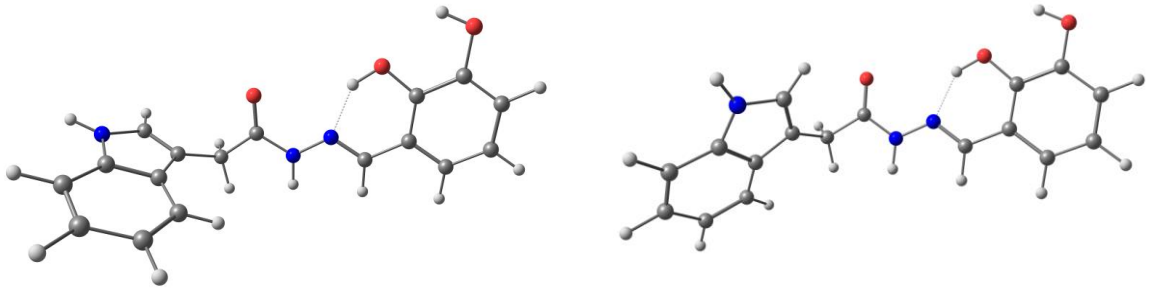

Conformer 1:

$\Delta G = 0$ kJ.mol^{-1}

Boltzmann population ratio = 75.54 %

Conformer 2:

$\Delta G = 3.10$ kJ.mol^{-1}

Boltzmann population ratio = 21.22 %

Figure 5. Optimized geometry of the two most stable conformers of compound *5a* in DMSO, Gibbs free energies, and Boltzmann distributions.

VI. In vivo evaluation in a scopolamine-induced model of Alzheimer's-type dementia in rats

The in vivo effects of the 3,4-dihydroxy derivative from the 5MICA series (compound **4b**) were investigated using behavioral and biochemical approaches, as detailed in publication B2. The compound was tested in a scopolamine-induced model of dementia in rats, with particular focus on its memory-enhancing potential, mechanisms of action, and toxicity profile. Rivastigmine, a reversible acetylcholinesterase inhibitor with clinical application in the treatment of mild-to-moderate Alzheimer's disease and various other forms of dementia (including Parkinson's disease-related dementia), was used as a positive control. Scopolamine, a non-selective muscarinic cholinergic receptor antagonist, served as a negative control. Scopolamine is known to induce memory impairments and cognitive deficits, accompanied by increased oxidative stress, neuroinflammation, alterations in monoaminergic neurotransmission, mitochondrial dysfunction, apoptosis, and impaired BDNF signaling—all hallmarks of Alzheimer's disease pathology. Therefore, this model was deemed suitable for evaluating compound **4b** as a potential candidate for the treatment of dementia and Alzheimer's disease.

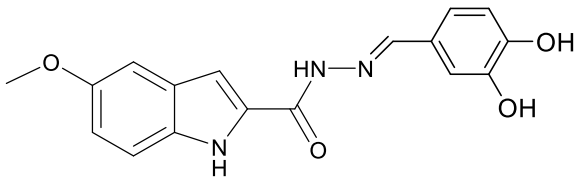

Figure 6. Molecular structure of the target compound N′-(3,4-dihydroxybenzylidene)-5-methoxy-1H-indole-2-carbohydrazide (4b).

VI.1. Behavioral assessment of the effects of 4b on learning and memory processes in rats

To assess the ability of compound **4b** to counteract the learning and memory deficits induced by scopolamine, two widely used behavioral paradigms were employed: the passive avoidance test and the Barnes maze.The step-through passive avoidance test is a classical method for evaluating memory in rodents, involving both emotional (aversive stimulus avoidance) and spatial components. Successful task performance depends largely on the functional integrity of the cholinergic system, particularly the release of acetylcholine from cholinergic neurons and its interaction with muscarinic acetylcholine receptors—notably in the hippocampus and prefrontal cortex.The Barnes maze is a validated method for assessing spatial learning and memory, likewise reliant on hippocampal function and muscarinic cholinergic signaling, especially activation of M1 muscarinic receptors in the hippocampus. As an antagonist of these receptors, scopolamine significantly impaired performance in both tasks compared to control animals.In the experiments conducted, scopolamine treatment disrupted task performance, resulting in a reduced step-through latency (STL) in the passive avoidance test 24 hours post-training, and a higher number of exploratory head dips in the Barnes maze.Treatment with compound **4b** fully restored STL values in scopolamine-treated animals to levels comparable with the control group. In the Barnes maze, 4b significantly reduced exploratory behavior (head dips) to control values, and its performance exceeded that of rivastigmine.

VI.2. Biochemical Evaluation of the Effects of 4b

To elucidate the mechanisms underlying the memory-enhancing effects of compound **4b**, its impact on the cholinergic system was assessed by measuring acetylcholine (ACh) levels and acetylcholinesterase (AChE) activity, alongside markers of oxidative stress, including lipid peroxidation and the enzymatic activity of superoxide dismutase (SOD), catalase (CAT), and glutathione peroxidase (GPx) in the cerebral cortex and hippocampus.

Acetylcholine plays a key role in memory formation and cognitive function, while acetylcholinesterase degrades ACh and is essential for proper cholinergic neurotransmission. It is well established that inhibition of AChE enhances memory and slows cognitive decline in patients with various forms of dementia. In the present model, scopolamine reduced ACh levels and increased AChE activity in both the hippocampus and cortex. Treatment with **4b** exerted a dual beneficial effect on the cholinergic system, increasing ACh levels while reducing AChE activity in the hippocampus, effectively restoring both parameters to control values.

Given the well-established link between oxidative stress and the progression of neurodegenerative diseases, as well as the in vitro data indicating the antioxidant potential of **4b**, it was deemed relevant to evaluate the compound's ability to modulate oxidative stress markers in vivo, particularly in relation to its observed cognitive benefits.

A particularly pronounced effect was observed on MDA levels and catalase activity. Scopolamine treatment led to a significant increase in MDA levels and a decrease in CAT activity. These pathological alterations were markedly attenuated by **4b**, which reduced MDA levels in the hippocampus to those of the control group, and even more prominently in the cerebral cortex, where MDA values were fully normalized. In contrast, rivastigmine had no effect on MDA levels, showing a biochemical profile identical to that of scopolamine.

As for catalase, 4b again outperformed rivastigmine, demonstrating a significant increase in catalase activity in the hippocampus, whereas no such increase was observed in the rivastigmine-treated group. Since catalase is the enzyme responsible for catalyzing the decomposition of H_2O_2 into water and oxygen, the observed in vivo elevation of scopolamine-suppressed catalase activity by **4b** is consistent with its neuroprotective action, previously established in cellular and subcellular models.These results were further supported by the effects of **4b** on GPx activity, an enzyme that also detoxifies H_2O_2 by reducing it to water. In the hippocampus, GPx activity in the presence of **4b** and scopolamine did not differ from control levels, whereas combined treatment with rivastigmine and scopolamine resulted in a significant reduction in GPx activity.

Although **4b** showed the strongest in vitro radical scavenging activity against superoxide radicals in our previous studies, it failed to restore scopolamine-reduced SOD activity in both the cortex and hippocampus in vivo. Rivastigmine was similarly ineffective, and in fact, SOD activity in the hippocampus was even lower than that observed in the **4b** group.

Brain-derived neurotrophic factor (BDNF) is a key neurotrophin that, in addition to its role in maintaining neuronal viability, growth, and differentiation, also plays an active role in synaptic plasticity, which underlies learning and memory. Data from various studies indicate that BDNF levels are reduced in the serum and cerebrospinal fluid of AD patients [15]. Conversely, higher serum BDNF levels in healthy elderly individuals correlate with a reduced risk of developing dementia. It has also been shown that BDNF and activation of the BDNF/TrkB signaling pathway can promote the non-amyloidogenic processing of amyloid precursor protein (APP) by stimulating α-secretase activity, thereby limiting β-amyloid production [16]. Moreover, BDNF influences the hyperphosphorylation of tau protein. Elevation of BDNF in the hippocampus is associated with attenuation of cognitive impairment and slowing of neurodegenerative processes.

In this context, the effect of **4b** on BDNF levels was investigated. Administration of **4b** successfully restored BDNF levels after scopolamine-induced depletion, bringing them close to those of the control group. This effect likely contributes to the positive influence of **4b** on memory consolidation, as observed in the behavioral tests for passive avoidance and the Barnes maze, both of which rely on activation of the BDNF/TrkB signaling pathway for successful task performance.

In addition to the investigation of **4b's** effects on learning, various types of memory, and their underlying mechanisms, its toxicity was also evaluated through the assessment of biochemical blood parameters, including ALAT, ASAT, creatinine, urea, albumin, globulin, and total protein.

The data demonstrated no adverse effects on liver or kidney function, thereby complementing the favorable safety profile of **4b**.

Therefore, the comprehensive pharmacological profile of **4b**, combined with its good tolerability and ability to cross the blood–brain barrier, suggests therapeutic advantages that may extend beyond symptomatic relief. The compound emerges as a promising candidate for further in-depth studies as a multi-target agent for the treatment of neurodegenerative disorders.

Perspectives for Future Research

Upcoming scientific work will focus on further investigation and optimization of the already identified structures with proven neuroprotective and antioxidant potential.

The synthesis of new potential multi-target compounds is planned, applying a rational design approach that combines established pharmacophoric fragments with novel promising pharmacophores, aiming at simultaneous modulation of several key pathological mechanisms involved in neurodegenerative diseases.

Selected molecules will be immobilized on functionalized nanoparticles in order to explore synergistic effects.

In vitro studies will be expanded using novel cellular models, to evaluate both the efficacy and mechanism of action of previously validated structures and new compounds.

New in vivo experiments are also planned with selected compounds and nanoparticles in models of Parkinson's and Alzheimer's disease, aiming to monitor behavioral outcomes and oxidative status.

In parallel, research will continue on the development of new antitumor agents, including hybrid molecules and nanoparticles with potential synergistic activity.

List of scientific publications submitted under indicator "B" for the competition for the academic position of Associate Professor

B1. Anastassova, N. ; Kondeva-Burdina, M. ; Hristova-Avakumova, N. ; Stefanova, D. ; Rangelov, M. ; Todorova, N. ; Yancheva, D. Exploring the Potential of Indole-3-acetic Acid Arylhydrazone Hybrids for Parkinson's Disease Treatment: A Comprehensive Evaluation of Neuroprotective, MAOB Inhibitory, and Antioxidant Properties, ACS Chem. Neurosci. 2025, available online. DOI: 10.1021/acschemneuro.4c00838

B2. Petkova-Kirova, P. ; Anastassova, N. ; Minchev, B. ; Uzunova, D. ; Grigorova, V. ; Tsvetanova, E. ; Georgieva, A. ; Alexandrova, A. ; Stefanova, M. ; Yancheva, D. ; Kalfin, R. ; Tancheva, L. Behavioral and Biochemical Effects of an Arylhydrazone Derivative of 5-Methoxyindole-2-Carboxylic Acid in a Scopolamine-Induced Model of Alzheimer's Type Dementia in Rats. Molecules 2024, 29, 5711. DOI: 10.3390/molecules29235711

B3. Anastassova, N. ; Stefanova, D. ; Hristova-Avakumova, N. ; Georgieva, I. ; Kondeva-Burdina, M. ; Rangelov, M. ; Todorova, N. ; Tzoneva, R. ; Yancheva, D. New indole-3-propionic acid and 5-methoxy-indole carboxylic acid derived hydrazone hybrids as multifunctional neuroprotectors, Antioxidants 2023, 12(4), 977. DOI: 10.3390/antiox12040977

B4. Anastassova, N.; Aluani, D.; Hristova-Avakumova, N.; Rangelov, M.; Todorova, N.; Kondeva-Burdina, M.; Tzankova, V.; Yancheva, D. 1,3-disubstituted benzimidazole arylhydrazones as new multi-target drug ligands for the treatment of Parkinson's disease with antioxidant action, Antioxidants2022, 11, 884. DOI: 10.3390/antiox11050884

B5. Anastassova, N.; Aluani, D.; Kostadinov, A.; Rangelov, M.; Todorova, N.; Hristova-Avakumova, N.; Argirova, M.; Lumov, N.; Kondeva-Burdina, M. ; Tzankova, V. ; Yancheva, D. Evaluation of the combined activity of benzimidazole arylhydrazones as new anti-Parkinsonian agents: monoamine oxidase-B inhibition, neuroprotection and oxidative stress modulation, Neural Regen Res 2021, 16(11), 2299. DOI: 10.4103/1673-5374.309843

References:

1. Dorsey, E. R., Sherer, T., Okun, M. S., & Bloem, B. R. (2018). The emerging evidence of the Parkinson pandemic. *Journal of Parkinson's Disease*, *8*(s1), S3–S8. https://doi.org/10.3233/JPD-181474

2. Kouli, A., Torsney, K. M., & Kuan, W. L. (2018). Parkinson's disease: Etiology, neuropathology, and pathogenesis. In Stoker, T. B., & Greenland, J. C. (Eds.), *Parkinson's Disease: Pathogenesis and Clinical Aspects* [Internet]. Brisbane (AU): Codon Publications. Chapter 1.

3. Terao, Y., Fukuda, H., Ugawa, Y., & Hikosaka, O. (2013). New perspectives on the pathophysiology of Parkinson's disease as assessed by saccade performance: A clinical review. *Clinical Neurophysiology*, *124*(8), 1491–1506. https://doi.org/10.1016/j.clinph.2013.01.021

4. Blesa, J., Trigo-Damas, I., Quiroga-Varela, A., & Jackson-Lewis, V. R. (2015). Oxidative stress and Parkinson's disease. *Frontiers in Neuroanatomy*, *9*, 91. https://doi.org/10.3389/fnana.2015.00091

5. Tong, J., Rathitharan, G., Meyer, J. H., Furukawa, Y., Ang, L. C., Boileau, I., Guttman, M., Hornykiewicz, O., & Kish, S. J. (2017). Brain monoamine oxidase B and A in human parkinsonian dopamine deficiency disorders. *Brain*, *140*(9), 2460–2474. https://doi.org/10.1093/brain/awx172

6. Imbriani, P., Martella, G., Bonsi, P., & Pisani, A. (2022). Oxidative stress and synaptic dysfunction in rodent models of Parkinson's disease. *Neurobiology of Disease*, *173*, 105851. https://doi.org/10.1016/j.nbd.2022.105851

7. Makhoba, X. H., Viegas Jr, C., Mosa, R. A., Viegas, F. P. D., & Pooe, O. J. (2020). Potential impact of the multi-target drug approach in the treatment of some complex diseases. *Drug Design, Development and Therapy*, *14*, 3235–3249. https://doi.org/10.2147/DDDT.S257494

8. Anastassova, N., Mavrova, A. Ts., Yancheva, D., Kondeva-Burdina, M., Tzankova, V., Stoyanov, S., Shivachev, B., & Nikolova, R. (2018). Hepatotoxicity and antioxidant activity of some new N,N′-disubstituted benzimidazole-2-thiones, radical scavenging mechanism and structure-activity relationship. *Arabian Journal of Chemistry*, *11*, 353–369.

9. Kitamura, Y., Kosaka, T., Kakimura, J. I., Matsuoka, Y., Kohno, Y., Nomura, Y., & Taniguchi, T. (1988). Protective effects of the antiparkinsonian drugs talipexole and pramipexole against 1-methyl-4-phenylpyridinium-induced apoptotic death in human neuroblastoma SH-SY5Y cells. *Molecular Pharmacology*, *54*, 1046–1054.

10. Student, A. K., & Edwards, D. J. (1977). Subcellular localization of types A and B monooxidase in rat brain. *Biochemical Pharmacology*, *26*, 2337–2342.

11. Sanyal, J., Bandyopadhyay, S. K., Banerjee, T. K., Mukherjee, S. C., Chakraborty, D. P., Ray, B. C., & Rao, V. R. (2009). Plasma levels of lipid peroxides in patients with Parkinson's disease. *European Review for Medical and Pharmacological Sciences*, *13*(2), 129–132.

12. De Lazzari, F., Bubacco, L., Whitworth, A. J., & Bisaglia, M. (2018). Superoxide radical dismutation as new therapeutic strategy in Parkinson's disease. *Aging and Disease*, *9*(4), 716–728.

13. Mehta, N. J., Asmaro, K., Hermiz, D. J., Njus, M. M., Saleh, A. H., Beningo, K. A., & Njus, D. (2016). Hypochlorite converts cysteinyl-dopamine into a cytotoxic product: A possible factor in Parkinson's disease. *Free Radical Biology and Medicine*, *101*, 44–52.

14. Anastassova, N. O., Yancheva, D. Y., Mavrova, A. T., Kondeva-Burdina, M. S., Tzankova, V. I., Hristova-Avakumova, N. G., & Hadjimitova, V. A. (2018). Design, synthesis, antioxidant

properties and mechanism of action of new N,N′-disubstituted benzimidazole-2-thione hydrazone derivatives. *Journal of Molecular Structure*, *1165*, 162–176.

15. Ng, T. K. S., Ho, C. S. H., Tam, W. W. S., Kua, E. H., & Ho, R. C. (2019). Decreased serum brain-derived neurotrophic factor (BDNF) levels in patients with Alzheimer's disease (AD): A systematic review and meta-analysis. *International Journal of Molecular Sciences*, *20*, 257. https://doi.org/10.3390/ijms20020257

16. Nigam, S. M., Xu, S., Kritikou, J. S., Marosi, K., Brodin, L., & Mattson, M. P. (2017). Exercise and BDNF reduce Aβ production by enhancing α-secretase processing of APP. *Journal of Neurochemistry*, *142*, 286–296. https://doi.org/10.1111/jnc.14094